

Static and dynamic optical nonlinearities in conjugated polymers: Third-harmonic generation and the dc Kerr effect in polyacetylene, polyparaphenylene vinylene, and polythienylene vinylene

Zhigang Shuai and J. L. Brédas

*Service de Chimie des Matériaux Nouveaux, Département des Matériaux et Procédés,
Université de Mons-Hainaut, place du Parc, 20, B-7000 Mons, Belgium*

(Received 9 September 1991; revised manuscript received 24 March 1992)

The static and dynamic second hyperpolarizability tensors of oligomers of polyacetylene, polyparaphenylene vinylene, and polythienylene vinylene are evaluated by means of the valence effective Hamiltonian (VEH) method. The sum-over-states (SOS) approach is exploited, by constructing excited states from both single- and double-electron excitations. The *ab initio* coupled perturbed Hartree-Fock method is also applied in the case of small representative molecules such as benzene, thiophene, styrene, and thienylethylene in order to test the validity of the VEH-SOS approach. The VEH-SOS results are found to be comparable with the *ab initio* results. The length dependence of the static hyperpolarizability is analyzed and found to scale with the optical gap evolution of the different oligomers. The dynamic properties are presented in terms of third-harmonic generation and the dc Kerr effect.

I. INTRODUCTION

Materials which exhibit strong optical nonlinear effects are essential for optronic or photonic devices. Conjugated polymers are found to present very large nonlinear optical responses.¹ Enormous attention, both theoretical and experimental, has therefore focused on trying to rationalize the origin of these responses, in order to design materials with optimal characteristics. Polyacetylene, which can be considered to be the prototype of conjugated polymers, to date possesses the largest third-order nonlinear optical coefficient $\chi^{(3)}$ among its class of compounds.²

The relevant microscopic mechanism for $\chi^{(3)}$ has been investigated with many approaches. In the context of correlated electron theory, Garito *et al.* have been able to calculate $\chi^{(3)}$ for short linear polyenes using a configuration interaction technique;³ Soos and Ramesha have carried out calculations based on the Pariser-Parr-Pople model and a diagrammatic valence-bond method;⁴ DeMelo and Silbey⁵ applied the variational method. The results of these calculations generally present some discrepancies with respect to the experimental data. For instance, (i) the two-photon resonance intensity is calculated to be either too weak (when it corresponds to a $2A_g$ resonance) or too strong (when it corresponds to a resonance with a higher-lying mA excited state, m depending on the oligomers and varying within the different methods); (ii) the frequency of the two-photon peak usually differs from the experimental value; (iii) the length-dependent saturation of the $\chi^{(3)}$ susceptibility is not satisfactorily reproduced, even for rather long polyenes containing up to 20 double bonds.^{5,6}

We note that recent contributions have provided a better description of the two-photon resonance behaviors. Dixit, Guo, and Mazumdar⁷ have suggested that the mA state always lies between the $1B$ and $2B$ states; as the chain length increases, the mA state becomes almost de-

generate with the $1B$ state, so that the two-photon resonance occurs exactly at half the optical gap (defined by the $1B$ state). This feature that the mA state is bonded between $1B$ and $2B$ is, however, not reproduced in other calculations.^{8,10} McWilliams and Soos¹¹ and Soos, *et al.*¹² have examined the influence of interchain coupling and concluded that three-dimensional (3D) dispersion effects can reduce the two-photon state energy and intensity (the exact amount of reduction depending on the coupling constant which is chosen). Correct evaluation of the saturation behavior remains, however, a problem.

On the other hand, there exist many approaches which rely on single-electron theory. In their pioneering work, Rustagi and Ducuing¹³ showed, on the basis of particle-in-a-box theory, that the second hyperpolarizability of a linear system has a length dependence as L^5 . In their early contributions, Hameka and co-workers¹⁴ applied Rayleigh-Schrödinger static perturbation theory based on Hückel molecular orbitals. They found a length dependence of $\gamma \sim N^{5.3}$ for hydrocarbon chains without any indication of saturation. Afterwards, McIntyre and Hameka¹⁵ constructed Slater determinants to describe the wave functions and found considerable improvement in comparison with their previous results when evaluating the static polarizability and hyperpolarizability of organic systems, including hydrocarbon chains, aromatics, and nitrogen compounds.

Recently, due to the enormous development of conjugated polymers, their nonlinear optical properties have been extensively investigated.¹ New theoretical approaches have been developed, including the instanton approach.¹⁶ Wu¹⁷ (by using a field-theoretical approach) and Wu and Sun¹⁸ (by improving the Genkin-Mednis method¹⁹) have obtained an analytic solution for the infinite one-dimensional (1D) polyacetylene system; however, the dynamic response, in particular the two-photon resonance they obtain, is much too weak in comparison

with the results of the free-electron laser experiments. The present authors have recently shown²⁰ that, when taking into account doubly excited states and an excitation-energy-dependent damping factor within a Su-Schrieffer-Heeger (SSH) Hamiltonian,²¹ reasonable results can be obtained, both for (i) the length dependence of the susceptibility (saturation of $\chi^{(3)}$ is found, which overcomes the drawbacks of the particle-in-a-box theory¹³ and simple Hückel theory¹⁴ and (ii) for the resonance features (position and relative intensities of three-photon and two-photon resonances). In this work, we develop the same kind of formulation as that successfully used in Ref. 20 and apply it to a valence effective Hamiltonian²² (VEH) description of the molecular orbitals (instead of a Hückel-type parametrization) in order to incorporate the details of the molecular structures. We construct the excited states on the same basis of single and double excitations from occupied to virtual VEH molecular orbitals. It is by now well established that the VEH reproduces very well the electronic properties of conjugated polymers, in particular what is related to the π and π^* levels, for instance the optical gap. The VEH also played an interesting role in materials design,²³ namely of low band-gap polymers.

We organize the paper in the following way. First, we

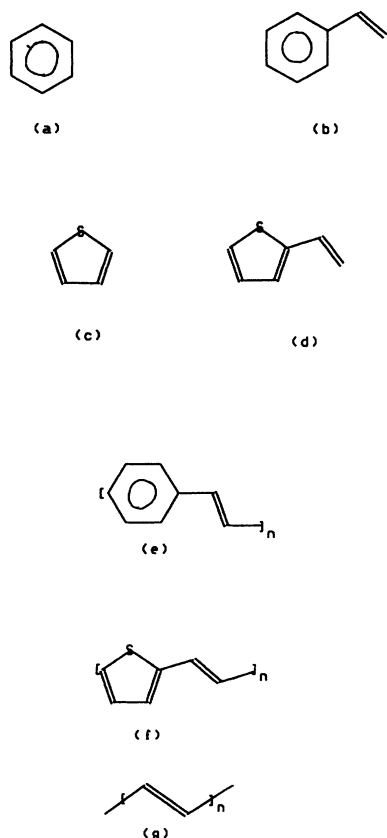


FIG. 1. Sketch of the molecular structures of (a) benzene, (b) styrene, (c) thiophene, (d) α -thienylethylene, (e) polyparaphenylene vinylene, (f) polythienylene vinylene, and (g) polyacetylene.

give a brief description of the VEH methodology, the sum-over-states (SOS) approach, and our formulation of transition moments and the summation procedure. We then present and discuss the results we have obtained when applying this methodology to the calculation of static and dynamic second-order hyperpolarizabilities in linear polyenes containing from four up to 30 carbons, as well as in oligomers of polyparaphenylene vinylene (PPV) and polythienylene vinylene (PTV) (see Fig. 1), two conjugated polymers of interest for their processibility and nonlinear optical responses. The *ab initio* coupled perturbed Hartree-Fock approach is also applied to study a number of small representative molecules such as benzene and thiophene and their vinylene derivatives, in order to make a comparison with the corresponding VEH-SOS results. The dynamic properties are evaluated in terms of third-harmonic generation (THG) and the dc-Kerr effect. The conclusions of our work are given in the last section.

II. METHODOLOGY

The method to obtain nonempirical one-electron valence effective Hamiltonians has been developed for molecules by Nicolas and Durand²⁴ and extended for polymers by André *et al.* and Brédas.²² The VEH technique is based on the construction of effective Fock operators F_{eff} ,

$$F_{\text{eff}} = -\frac{\Delta}{2} + \sum_A V_A, \quad (1)$$

which includes the kinetic term and a sum over the various atomic potentials in the system. These effective atomic potentials V_A explicitly include nuclear attraction, Coulomb repulsion, and exchange since they have been parametrized by optimizing the eigenvalues of Fock operators for each type of atom to reproduce *ab initio* double- ζ quality calculations on model molecules (including ethane, butadiene, and acetylene for carbon,²⁵ and thiophene and dimethylsulfide for sulfur.²⁶) The basis set which is used is of minimal type but, in conjunction with the parametrization of the atomic potentials, produces one-electron energy levels of double- ζ quality.²² Only valence electrons are explicitly considered and one-electron integrals need to be evaluated, which allows one to carry out calculations on large-size molecules. As mentioned in the Introduction, previous calculations on a wide range of conjugated polymers^{22(b)} and macrocycles²⁷ have shown that VEH affords very good estimate for π - π^* band gaps.

For determining nonlinear optical susceptibilities, one is concerned with the response of a (molecular) system with respect to an external time-dependent electric field (that of a laser, for instance) and has the choice between derivatives or perturbative techniques.^{1(c)} In the finite-field approach,²⁸ one evaluates the variation of total energy of the system in presence of a static (finite) electric field, followed by a numerical differentiation which provides the (hyper)polarizability components; in the coupled perturbed Hartree-Fock (CPHF) method,²⁹ one

deals with an analytical differentiation of the Hartree-Fock-Roothan equations with respect to electric field. Perturbative techniques are represented by the sum-over-states approach,³⁰ where time-dependent high-order perturbation theory is applied directly to evaluate the response of the system to an applied field.

Here, we develop our formulation of the SOS ap-

proach. The unperturbed molecular eigenstates are constructed by Slater determinants of VEH molecular orbitals, i.e., one-determinant configurations based on both single- and double-electron excitations from VEH occupied molecular orbitals to virtual molecular orbitals. Within the SOS approach discussed by Orr and Ward,³⁰ the second hyperpolarizability γ is expressed as

$$\begin{aligned} \gamma_{\alpha\beta\gamma\delta}(-\omega_\sigma; \omega_1, \omega_2, \omega_3) &= (h/2\pi)^{-3} k(-\omega_\sigma; \omega_1, \omega_2, \omega_3) \\ &\times \left[\sum_p \left[\sum_{m,n,p(\neq g)} \frac{\langle g|\mu_\alpha|m\rangle \langle m|\mu_\beta|n\rangle \langle n|\mu_\gamma|p\rangle \langle p|\mu_\delta|g\rangle}{(\omega_{mg}-\omega_\sigma-i\Gamma_{mg})(\omega_{ng}-\omega_1-\omega_2-i\Gamma_{ng})(\omega_{pg}-\omega_1-i\Gamma_{pg})} \right] \right. \\ &\left. - \sum_p \left[\sum_{m,n(\neq g)} \frac{\langle g|\mu_\alpha|m\rangle \langle m|\mu_\beta|g\rangle \langle g|\mu_\gamma|n\rangle \langle n|\mu_\delta|g\rangle}{(\omega_{mg}-\omega_\sigma-i\Gamma_{mg})(\omega_{ng}-\omega_1-i\Gamma_{ng})(\omega_{ng}+\omega_2+i\Gamma_{ng})} \right] \right]. \end{aligned} \quad (2)$$

In this expression, $\omega_\sigma = \omega_1 + \omega_2 + \omega_3$ is polarization response frequency; $\omega_1, \omega_2, \omega_3$ indicate the frequencies of the perturbing radiation fields (for third-harmonic-generation processes, $\omega_1 = \omega_2 = \omega_3 = \omega$; for the dc Kerr effect, $\omega_1 = \omega_2 = 0, \omega_3 = \omega$); \sum_p indicates a summation over the 24 terms obtained by permuting the frequencies; the numerical factor K is chosen as $\frac{1}{6}$ so that in the static case or for THG, only four terms are kept in Eq. (2), in agreement with other formulations;^{3,31} m, n , and q denote excited states and g , the ground state (all states correspond to single Slater determinants); μ_α is the α ($=x, y, z$) component of the dipole operator; ω_{ng} is the transition frequency between the n and g states, and Γ_{ng} is the damping factor for excited state n which is taken as excitation energy dependent.²⁰ Following Lalama and Garito³² and McIntyre and Hameka,¹⁵ the transition moments write

$$\langle g|er|m\rangle = \sqrt{2} \int dr \psi_s^*(r) er \psi_i(r), \quad (3)$$

$$\begin{aligned} \langle m|er|n\rangle &= \int dr \psi_s^*(r) er \psi_i(r) \delta_{ij} \\ &- \int dr \psi_i^*(r) er \psi_j(r) \delta_{st}. \end{aligned} \quad (4)$$

In these expressions, $|g\rangle = D_0$ denotes the ground state with doubly occupied valence levels; $|m\rangle = D_{i \rightarrow s}$, $|n\rangle = D_{j \rightarrow t}$, where indices i, j indicate occupied levels and indices s, t virtual level; $D_{i \rightarrow s}$ then refers to the Slater

determinant (electron configuration) where one electron has been promoted from occupied level i to virtual levels s ; er is the one-electron dipole operator, hence $|m\rangle$ and $|p\rangle$ in Eq. (2) have to correspond to singly excited configurations; on the other hand, $|n\rangle$ can also correspond to a doubly excited configuration: $|n\rangle = D_{i \rightarrow s, j \rightarrow t}$. We note that for each $|m\rangle$ configuration, there can occur three kinds of $|n\rangle$ configurations producing nonzero transition moments. For instance, for $|m\rangle = D_{i \rightarrow s}$: (i) $|n\rangle = D_{i \rightarrow t}$, (ii) $|n\rangle = D_{j \rightarrow s}$; and (iii) $|n\rangle = D_{i \rightarrow s, j \rightarrow t}$. For $|p\rangle$, the situation is analogous, in order to yield nonzero $\langle p|er|n\rangle$ transition moments. We follow McIntyre and Hameka¹⁵ to evaluate the double excitations channels. In Table I, we summarize the summation processes corresponding to the first term in Eq. (2).

In the linear combination of atomic orbitals (LCAO) approximation, the molecular orbitals are expressed in terms of basis functions χ_k ,

$$\psi_i(r) = \sum_k c_{1k} \chi_k(r - r_k) \quad (5)$$

so that

$$\begin{aligned} \int dr \psi_s^*(r) er \psi_i(r) &= \sum_{k,k'} C_{sk}^* C_{ik'} \int dr \chi_k^*(r - r_k) \\ &\times er \chi_{k'}(r - r_{k'}). \end{aligned} \quad (6)$$

TABLE I. Synopsis of the summation processes corresponding to the first term of Eq. (2), which can provide nonzero transition moments. Indices i, j, k refer to occupied levels and indices r, s, t to virtual levels. The table indicates that in the summation process, when one chooses an excited state for $|m\rangle$ (first line), there are three kinds of $|n\rangle$ states (second line) needed to be considered in connection with $|m\rangle$ and, corresponding to the three $|n\rangle$ states, there is a total of eight $|p\rangle$ states, as explained in the text.

$ m\rangle = D_{j \rightarrow s}$		$ m\rangle = D_{i \rightarrow t}$		$ m\rangle = D_{i \rightarrow s}$		$ m\rangle = D_{i \rightarrow s, j \rightarrow t}$	
$ p\rangle = D_{j \rightarrow t}$	$ p\rangle = D_{k \rightarrow s}$	$ p\rangle = D_{i \rightarrow r}$	$ p\rangle = D_{j \rightarrow t}$	$ p\rangle = D_{i \rightarrow s}$	$ p\rangle = D_{j \rightarrow t}$	$ p\rangle = D_{i \rightarrow t}$	$ p\rangle = D_{j \rightarrow s}$
γ_4	γ_3	γ_2	γ_1	γ_5	γ_6	γ_7	γ_8

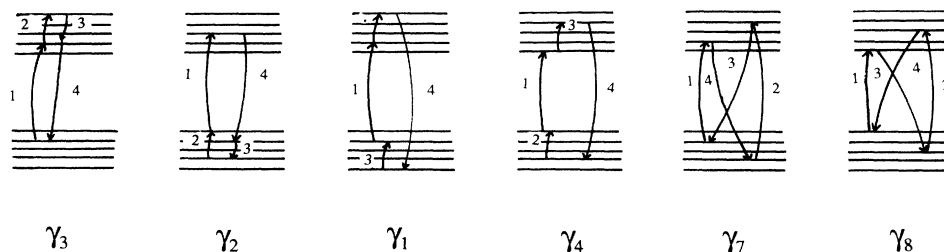


FIG. 2. Illustration of the relevant contributions to γ , following the notation of Table I. Note that in systems with charge conjugation symmetry: $\gamma_2 = \gamma_3$, $\gamma_1 = \gamma_4$, $\gamma_7 = \gamma_8$.

From Table I we observe there are eight types of possible contributions to the first term of Eq. (2). We stress that the second term of Eq. (2) only deals with single excitations $|m\rangle$ and $|n\rangle$ being independent from one another; this corresponds to an unlinked process. We note that γ_5 and γ_6 (see Table I) also correspond to unlinked processes (related to double excitations). It has been shown that all the unlinked processes cancel exactly (Wick's theorem).^{33,20} The remaining relevant contributions to γ are illustrated in the diagram of Fig. 2, which can be compared with the fourth-order Rayleigh-Schrödinger perturbation diagram.³⁴ Note that in any perturbation expansion, only the linked diagrams should eventually be kept, otherwise, there occur volume dependence problems (or, in the one dimension case, length dependence problems, as in previous studies.^{13,14})

From our recent SSH-SOS calculations,²⁰ we find that the γ_2 and γ_3 contributions are positive, while the γ_1 and γ_4 terms are negative; γ_7 and γ_8 are negative, but very small in magnitude for large systems. We note that each process depicted in Fig. 2 has a large size dependence, but the compensation between the positive and the negative terms makes the total γ value to evolve linearly when the system size is large enough, i.e., when it exceeds the effective conjugation length for nonlinear optical processes

(for instance, for linear polyenes, when $N \sim 50$, as was shown previously).^{3,20}

III. RESULTS AND DISCUSSION

A. THG and dc Kerr effect in linear polyenes

Linear polyenes have been studied in many ways³⁵ and recently very much in terms of their third-order susceptibilities, which range among the largest ever measured. The infinite-chain limit, polyacetylene, even constitutes the first example of a wide-frequency dispersion THG spectrum measurement.² In this section we investigate linear polyenes ranging in size from $N = 4$ to 30.

We fully optimized the geometry of all trans-butadiene ($N = 4$) and hexatriene ($N = 6$) with the Hartree-Fock semiempirical AM1 (Austin Model 1) technique;³⁶ the geometry of the longer polyenes were simply obtained by extending the central portion of hexatriene. We then applied the VEH to obtain the valence electronic structure and the transition moments [see Eqs. (3)–(6)], and summed over the six diagrams depicted in Fig. 2 to calculate γ . In the case of third-harmonic-generation (THG), γ is expressed as $\gamma(-3\omega; \omega, \omega, \omega)$, while for the dc Kerr effect, $\gamma(-\omega; 0, 0, \omega)$, see Eq. (2). In the static case where

TABLE II. Static second-hyperpolarizability averaged γ value (10^{-36} esu) for polyenes ($N = 4-30$). We also list the VEH band gap E_g (eV) for each molecule in the last entry and provide a comparison with the γ values calculated at the SSH-SOS (Ref. 20), MNDO finite-field (Ref. 38) and Hartree-Fock *ab initio* (Ref. 37) levels. The *ab initio* results are given for the minimal STO-3G basis set, the split-valence 6-31G basis set, and a 6-31G basis set augmented by polarization (P) and diffuse (D) functions (Ref. 37).

N	VEH	SSH-SOS	MNDO-FF	STO-3G	6-31G	6-31G + PD	E_g
4	0.51	1.36	2.14	0.25	0.55	7.48	5.41
6	6.42	14.20	15.18	2.74	4.97	17.69	4.13
8	36.70	59.34	52.06	11.33	20.54	41.41	3.49
10	127.50	163.42	125.45	31.12	57.73	89.87	3.08
12	333.55	349.16	243.30	66.69	127.85	174.13	2.78
14	721.20	628.90	408.15	120.90	239.94	303.98	2.59
16	1358.62	1003.40	618.27	197.47	407.40	491.71	2.43
18	2305.96	1464.36	869.25	290.29	619.66		2.32
20	3608.00	1998.52	1155.95	405.38	896.76		2.22
22	5295.17	2590.92	1472.84	526.39	1198.92		2.14
24	7374.19	3227.44	1814.86				2.08
26	9838.30	3896.22	2178.10				2.03
28	12 664.93	4587.58	2558.32				1.98
30	15 826.55	5294.38	2952.42				1.93

$\omega=0$, there is of course no difference between the various nonlinear optical processes. We present in Table II the evolution of the static γ values from $N=4$ to 30, and for comparison, the *ab initio* coupled perturbed Hartree-Fock results of Hurst, Dupuis, and Clementi³⁷ (with three different basis sets), the semiempirical modified neglect of differential overlap (MNDO) finite-field results of Kurtz,³⁸ and our previous Hückel-type results.²⁰ The average γ is defined as $\gamma=(\gamma_{xxxx} + \gamma_{yyyy} + 2\gamma_{xxyy})/5$, where we have neglected the z component (z is the axis perpendicular to the molecular plane) due to the planar character of the molecular structure.

The VEH-SOS results for small-sized ($N=4,6$) systems are comparable to the *ab initio* 6-31G results. This is not unexpected since the VEH parametrization has been carried out to reproduce an electron energy level of double- ζ quality.^{24,25} For large systems, the VEH-SOS γ values increase faster but remain within the same order of magnitude as the 6-31G *ab initio* values. It should be stressed that, as chain length increases, the 6-31G results gain in quality relative to the 6-31G + PD results (since atomic basis functions on distant sites allow for a simulation of diffuse functions.³⁷) The VEH-SOS approach can thus be expected to work well in long oligomers, which is precisely the objective we were aiming at in developing the technique.

It is interesting to point out that our SSH results are close to the *ab initio* 6-31G + PD results for short and intermediate lengths and are comparable for the long chains to the MNDO values (within a factor of 2). For very long chains (polyacetylene), the SSH results of $\chi^{(3)}$ quantitatively agree with the measured values. To show this, we calculate γ for the $N=200$ polyene; γ_{xxxx} is found to be 3.75×10^{-31} esu. Following Yu *et al.*,¹⁶ we then consider (i) a local-field correction for solid polyacetylene $f_L=10$, (ii) a chain number density (per cross section) $\sigma=3.2 \times 10^{14}$ /cm², and (iii) a one-dimensional lattice constant $c=1.22$ Å. The $\chi^{(3)}$ value is expressed as $\chi^{(3)}=f_L \sigma \gamma_{xxxx} / (5Nc)=9.84 \times 10^{-11}$ esu, where the factor $\frac{1}{5}$ is taken from random orientation average; for a well-oriented system, this factor is $\frac{3}{8}$ and our averaged

value for $\chi^{(3)}$ then amounts to 1.85×10^{-10} esu. These two estimates are in excellent agreement with the free-electron laser measurements by Fann *et al.*² for THG in polyacetylene ($\chi^{(3)} \sim 2 \times 10^{-10}$ esu in off-resonance conditions).

The faster increase of the VEH γ values can be rationalized in terms of the band-gap evolution. In the SSH model, the parameters have been chosen to reproduce the gap of the polymer to be 1.8 eV,²⁰ and the "gap" of the polyene molecules rapidly approaches the asymptotic value. On the other hand, on the basis of the AM1-optimized geometries (which provide a degree of bond-length alternation of 0.11 Å in the middle of the molecules), the VEH method leads to a band gap for polyacetylene of 1.4 eV. The effective conjugation length is thus longer with VEH than within our previous SSH approach; the γ values are accordingly bigger if we follow the argument of Agrawal, Cojan, and Flytzanis³⁹ that the nonresonant $\chi^{(3)}$ value scales as one over the sixth power of the band gap. If we represent γ as $\gamma \sim N^{a(N)}$ (evidently the value of a is dependent on N , rather than being a constant), we obtain that the a value (from fitting to the local slope of the logarithm of γ) with the VEH method varies from 6.0 for $N=6$ to 3.3 for $N=30$, while for the SSH-SOS calculations,²⁰ it varies from 5.7 to 1.6, thereby more rapidly approaching the saturation regime, i.e., one. We note that in the recent SSH-SOS work of Yu and Su,³¹ γ reaches 4000×10^{-36} esu for $N=20$ (which is even bigger than our VEH 3608×10^{-36} esu value) and the saturation behavior occurs around 80 carbon sites in those calculations. As is known, the original SSH parameters²¹ give a polymer gap of 1.4 eV.

The saturation behavior in the case of the first-order polarizability α is different. We present in Table III the α results for linear polyenes. The VEH-SOS averaged α value is defined as $\alpha=1/3(\alpha_{xx} + \alpha_{yy})$, neglecting again the perpendicular components. We see that the VEH-SOS results for α are similar to the results of other approaches for small and intermediate chain lengths; in the case of long chains, the VEH-SOS α values are within a factor of 2 relative to the MNDO results. The saturation

TABLE III. Values of α for linear polyenes (in 10^{-24} esu). Comparison is provided between the results of the VEH-SOS approach and those from other techniques as detailed in the caption of Table II.

N	VEH	MNDO-FF	STO-3G	6-31G	6-31G + PD
4	5.50	8.15	3.79	3.34	7.88
6	11.07	13.43	6.75	10.82	13.01
8	20.60	19.52	10.37	16.26	19.09
10	30.97	26.21	14.53	22.52	26.00
12	42.94	33.35	19.09	29.44	33.57
14	56.70	40.79	23.93	36.84	41.63
16	71.90	48.47	29.09	44.87	50.30
18	86.69	56.32	34.31	53.01	
20	103.25	64.28	39.75	61.62	
22	119.16	72.34	45.08	70.04	
24	136.45	80.46			
26	153.69	88.63			
28	171.10	96.84			
30	188.08	105.08			

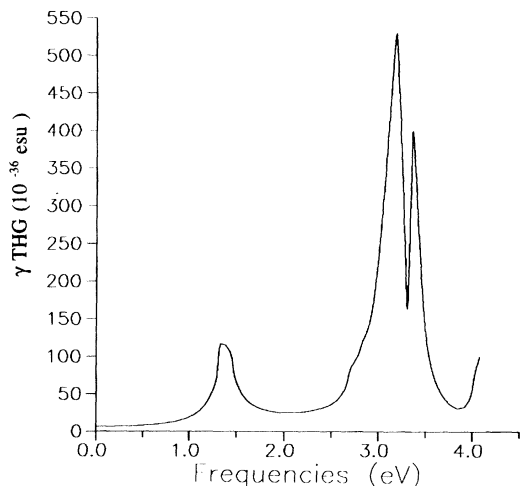


FIG. 3. VEH-SOS theoretical THG spectra for hexatriene ($N=6$).

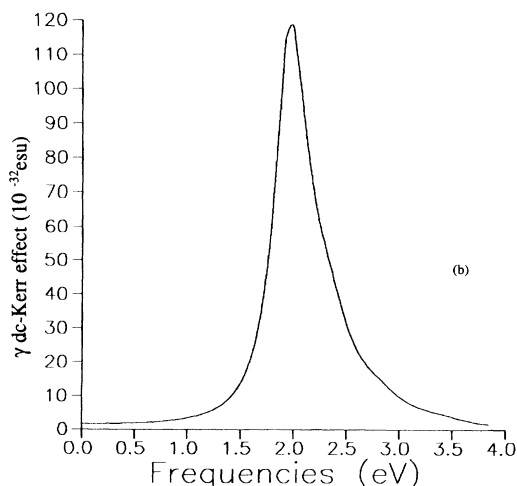
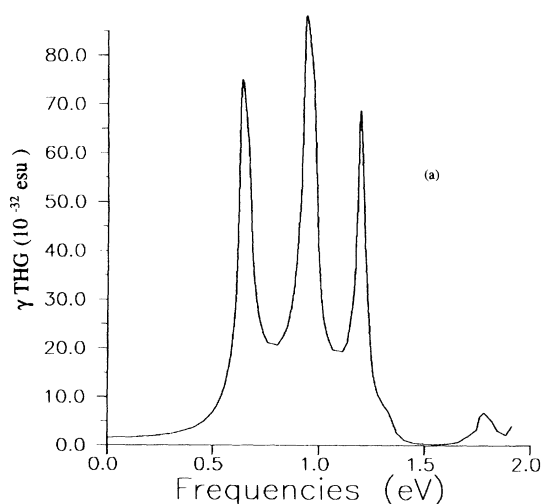


FIG. 4. VEH-SOS theoretical γ spectra for polyene with ($N=30$) carbons: (a) THG; (b) dc Kerr effect.

almost already occurs within the chain lengths considered in the present calculations: $\alpha \sim N^{b(N)}$, the b value going from 2.1 for $N=6$ to 1.2 for $N=30$. This behavior that the critical length (of saturation) for α is shorter than that for γ , as obtained with our VEH method, agrees with previous calculations,³⁻⁵ but contradicts the recent calculations of Kavanaugh and Silbey,⁴⁰ in the latter work, however, only nearest-neighbor interactions are effectively taken into account, a feature which might underestimate the delocalization characteristics of the third-order response.

The VEH-SOS frequency-dependent spectra for $N=6$ and 30 are shown in Figs. 3 and 4. In Figs. 3 and 4, the resonant features are associated with the details of the electronic structure. For example, in Fig. 4(a), there are three peaks in the THG process which correspond to $1B_u$, $2B_u$, and $2A_g$ resonances, the former two being three-photon resonances and the latter one being two-photon resonance. In the long-chain limit, the first two peaks merge, as seen in the SSH-type calculation for $N=200$.²⁰ In Fig. 4(b) the dc Kerr effect spectrum is less structured, since it is difficult to distinguish between the various types of resonances; indeed when, for instance, B_u and A_g configurations appear at about the same energies, it is always possible to consider $\omega=0$ photons (static field) to change the symmetry of the resonance. For all the calculations of these spectra, we have adopted the excitation-energy-dependent damping factor Γ_{ng} .²⁰ In Fig. 4(b) for the dc Kerr effect, we have applied a bigger damping factor (which is set to be 0.15 times the excitation energies) than for the THG case (0.04 times the excitation energies), since the one-photon resonance [see Eq. (2)] is much stronger than multiphoton peaks; as a result, the curve in Fig. 4(b) is quite smooth, consisting of one broad peak covering $1B_u$, $2A_g$, and $2B_u$ resonances, which are close in energies.

B. THG and dc Kerr effect in oligomers of polyparaphenylene vinylene

We have carried out the VEH-SOS calculations for benzene, styrene, and phenylcapped oligomers of polyparaphenylene vinylene, going from the monomer ($N=1$, corresponding to trans-stilbene) up to the tetramer ($N=4$). For comparison with higher-level calculations, we have also performed coupled perturbed Hartree-Fock *ab initio* 6-31G* calculation for benzene and styrene. The polarizability and second hyperpolarizability results are presented in Table IV. There is good agreement for both α and γ between the results of the two techniques. We stress that there occurs a large in-

TABLE IV. VEH-SOS and CPHF *ab initio* results of polarizability α and second hyperpolarizability γ for benzene and styrene (α in 10^{-24} esu and γ in 10^{-36} esu).

	α		γ	
	VEH-SOS	6-31G*	VEH-SOS	6-31G*
Benzene	7.78	7.72	0.31	0.48
Styrene	10.81	11.31	3.37	2.54

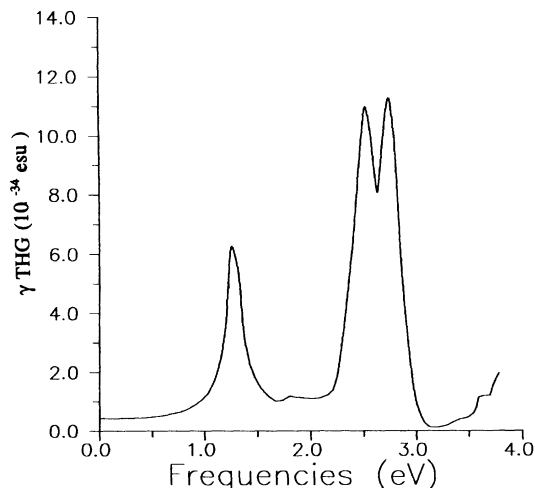


FIG. 5. VEH-SOS theoretical THG spectra for stilbene ($N=1$).

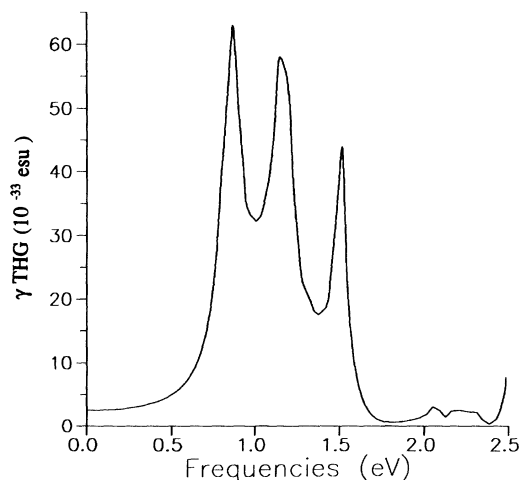


FIG. 6. VEH-SOS theoretical THG spectra for the PPV tetramer ($N=4$).

crease of γ (about one order of magnitude) in going from benzene to styrene while the α values evolve by only some 50%. We will discuss this feature later.

For the PPV oligomers, the VEH calculations are based on the AM1-optimized geometry of stilbene ($N=1$). For larger systems, we simply extend the stilbene geometric structure. Note that there appear a number of (almost) degenerate electronic levels, due to electronic wave functions localized within the benzene rings; in the polymer, these electronic levels give rise to the very flat (dispersionless) HOMO-1 and LUMO+1 bands.⁴¹ The static second-order hyperpolarizabilities are presented in Table V.

The exponential dependence of the second hyperpolarizability ($\gamma \sim N^a$) shows a saturation behavior within the range of oligomers considered in this work; the power value a goes from 4.8 to 2.8, which is similar to the SSH-Hückel results (from 4.7 to 2.6). The spectra for THG are given in Figs. 5 and 6 for the $N=1$ and 4 oligomers. The THG features in Figs. 5 and 6 are similar in character to those of the $N=6$ and 30 polyenes. We do not give the corresponding figures for the dc Kerr effect, since the structure is the same as in the case of polyenes, i.e., consisting of one strong peak. Note that when examining the γ features below 6 eV, no contribution is found from the electronic levels localized within the benzene rings, i.e., there are no peaks corresponding to the degenerate π levels.

A comparison can be made of the magnitudes of the static hyperpolarizabilities between linear polyenes and PPV oligomers when taking the $N=3$ PPV oligomer (which contains 30π electrons) and $C_{30}H_{32}$. We calculate that the value for the polyene chain is more than one order of magnitude (16 times) larger than for the PPV compound. This agrees with the measured data, in that the off-resonance $\chi^{(3)}$ of polyacetylene is about 10^{-10} esu,² while that of PPV is on the order of 5×10^{-12} esu ($\omega=0.58$ eV).⁴² This feature that the γ values decrease in going from linear molecules to ring-containing systems has been demonstrated previously by Li *et al.*⁴³ Simply using the $(1/E_g^6)$ dependence³⁹ would have provided only a factor of 8 as the difference between $C_{30}H_{32}$ and the $N=3$ PPV oligomer.

C. THG and the dc Kerr effect in oligomers of polythienylene vinylene

Like PPV,^{41,44} poly(2,5-thienylene vinylene) (PTV) is a conjugated polymer of high current interest for nonlinear optical studies, in particular because of its processibility into thin films and its high environmental stability. PTV is reported⁴⁵ to display a magnitude for the dc Kerr $\chi^{(3)}(-\omega;0,0,\omega)$ susceptibility similar to that of polyacetylene and polydiacetylene.

We first investigate the polarizabilities of thiophene

TABLE V. VEH-SOS components of γ (10^{-36} esu) for phenyl-capped PPV oligomers. The results of our previous SSH-Hückel calculations are included. The x axis is the direction of the polymer chain. The VEH-SOS first-order polarizability α (in 10^{-24} esu) and VEH gap (eV) are given for each oligomer.

N	E_g	γ_{xxxx}	γ	γ_{xxxx} (SSH)	α	No. of carbons
1	3.81	184.67	42.63	136.26	22.57	14
2	3.11	1520.03	326.06	1157.62	44.86	22
3	2.81	4886.22	961.57	3363.04	66.32	30
4	2.65	9777.14	1923.41	6666.66	89.53	38

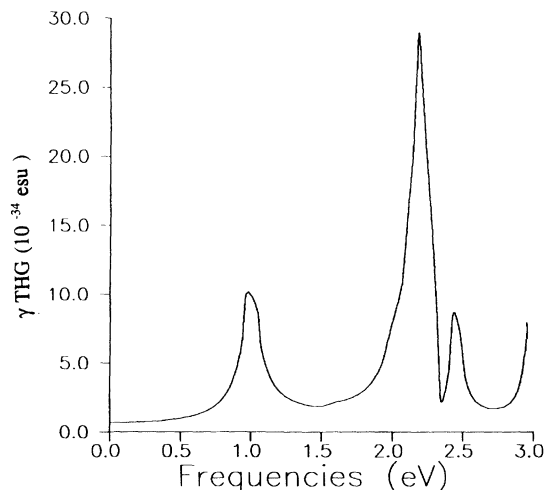


FIG. 7. VEH-SOS theoretical THG spectra for the $N=1$ PTV oligomer.

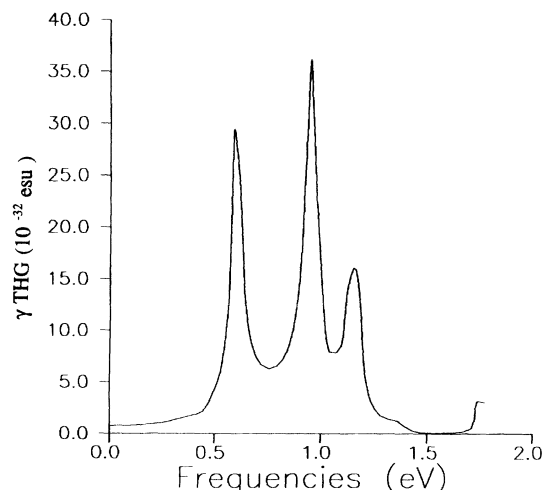


FIG. 8. VEH-SOS theoretical THG spectra for the $N=4$ PTV oligomer.

and α -thienylethylene, with both VEH-SOS and CPHF *ab initio* 6-31G* methods. The results are given in Table VI. Again we observe that, as for benzene and styrene, α evolves much less than γ when attaching an ethylenic moiety to the aromatic ring. We have also considered thienyl-capped PTV oligomers from $N=1$ to 4 (the $N=1$ compound thus corresponding to 1,2-dithienyl-ethylene). As in the previous cases, geometry optimization of the $N=1$ oligomer is carried out by the semiempirical AM1 method. We calculated the static and dynamic second-order hyperpolarizabilities and their evolution with increasing size of the molecules, see Figs. 7 and 8. The static results are listed in Table VII.

The magnitude of the static γ is consistently larger for the PTV oligomers than for the PPV oligomers. For instance, for $N=4$, the PTV γ is about four times bigger. When we compare to the polyene compounds, taking into account the number of π electrons, the PTV oligomers present static γ values that are about five times lower. For instance, the $N=3$ PTV (30π electrons) static γ is 2868.9×10^{-36} esu to be compared to 15826.5×10^{-36} esu for the $N=30$ polyene. It is of interest to point out that, based on the simple $1/(E_g)^6$ dependence of γ derived by Agrawal, Cojan, and Flytzanis,³⁹ the $N=3$ PTV value should have amounted to about the same value as that of the $N=30$ polyene.

It is most important stressing the following feature. The first-order polarizabilities of styrene or polypara-phenylene oligomers are found to be larger than those of

thienylethylene or polythiophene oligomers.⁴⁶ As we obtain in the present work and in agreement with experimental data, the magnitude of the third-order polarizability is, however, significantly greater for the thiophene derivatives than the phenylene derivatives. The main consequences are the following: (i) the scaling laws that have been used to extrapolate α values to γ values have to be taken with much caution; (ii) aromaticity (which is larger for benzene than thiophene) is not detrimental to first-order polarizability, as this remains a rather local effect (note that even in linear polyenes, α saturates much more rapidly than γ does); however, strong aromaticity obviously appears to be a drawback when considering higher-order polarizabilities, being it β (Refs. 47 and 48) or γ .

IV. SYNOPSIS

In summary, we have evaluated the second hyperpolarizabilities of linear polyenes and oligomers of PPV and PTV within a VEH sum-over-states approach. The VEH-SOS technique appears to be a useful method to describe the nonlinear optical properties of chains containing up to 40–50 carbons. By including doubly excited configuration channels, we have been able to provide a smooth length-dependent saturation. Among the three types of compounds we have studied, the linear polyenes present the largest third-order polarizabilities; for systems containing on the order of 30π electrons, the static

TABLE VI. VEH-SOS and CPHF *ab initio* results of polarizability α and second hyperpolarizability γ for thiophene and α -thienylethylene (α in 10^{-24} esu and γ in 10^{-36} esu).

	α		γ	
	VEH-SOS	6-31G*	VEH-SOS	6-31G*
Thiophene	5.47	7.06	0.22	0.43
Thienylethylene	10.90	10.68	3.46	2.30

TABLE VII. VEH-SOS static γ components for the thienyl-capped PTV oligomers (in 10^{-36} esu). The VEH-SOS first-order polarizability α (in 10^{-24} esu) and VEH gap (eV) are given for each oligomer.

N	E_g	γ_{xxxx}	γ	α	No. of π electrons
1	3.00	304.51	67.90	27.07	14
2	2.26	3419.38	682.56	58.66	22
3	1.96	14 375.08	2868.90	97.11	30
4	1.80	37 689.30	7527.03	138.94	38

γ values of polyenes are about 16 and 5 times larger than those of the corresponding PPV and PTV oligomers, respectively. A simple application of the $(1/E_g^6)$ relationship derived by Agrawal, Cojan, and Flytzanis would have provided significantly smaller differences (factors of 8 and 1, respectively).

When comparing PPV and PTV, polythiethylene vinylene oligomers provide a bigger nonlinear optical response. This can be related to the lower aromaticity of thiophene with respect to benzene; a better delocalization of charge outside of the rings along the chain can therefore be achieved in PTV. This feature is also present in the results of our *ab initio* CPHF calculations for benzene, thiophene, styrene, and α -thienylethylene. We pointed out that one has to be very careful when applying scaling laws to extrapolate α values to γ values, as trends can become inverted when going from first-order polarizability (which has a more local character) to second- or third-order polarizabilities (which require extensive delocalization).

ACKNOWLEDGMENTS

We thank SPPS (Service de Programmation de la Politique Scientifique, "Programme d'Impulsion en Technologie de l'Information", Grant No. IT/SC/22), FNRS (Fonds National Belge de la Recherche Scientifique), and IBM-Belgium for the use of the Belgian Supercomputer Network. This work is partly supported by the Belgian "Pôle d'Attraction Interuniversitaire No. 16: Chimie Supramoléculaire et Catalyse," and an IBM Academic Joint Study, and by the Commission of European Community programme BRITE (Basic Research of Industrial Technology for Europe)/EURAM (European Research on Advanced Materials) Project No. 0148 NAPOLEO (Novel Applications of Polymers in Electronics and Optics). We thank C. Adant for carrying out the 6-31G* calculations⁴⁹ on benzene, styrene, thiophene, and thienylethylene.

- ¹(a) *Nonlinear Optical Properties of Organic Molecules and Crystals*, edited by D. S. Chemla and J. Zyss (Academic, Orlando, 1987); (b) *Conjugated Polymeric Materials: Opportunities in Electronics, Optoelectronics, and Molecular Electronics*, edited by J. L. Brédas and R. R. Chance, Vol. 18 of *NATO Advanced Study Institute, Series E* (Kluwer, Dordrecht, 1990); (c) P. N. Prasad and D. J. Williams, *Introduction to Nonlinear Optical Effects in Molecules and Polymers* (Wiley, New York, 1991). (d) *Organic Molecules for Nonlinear Optics and Photonics*, edited by J. Messier, F. Kajzar, and P. Prasad, Vol. 194 of *NATO Advanced Study Institute, Series E* (Kluwer, Dordrecht, 1991); (e) *Conjugated Polymers: The Novel Science and Technology of Highly Conducting and Nonlinear Optically Active Materials*, edited by J. L. Brédas and R. Silbey (Kluwer, Dordrecht, 1991).
- ²W.-S. Fann, S. Benson, J. M. J. Madey, S. Etemad, G. L. Baker, and F. Kajzar, *Phys. Rev. Lett.* **62**, 1492 (1989).
- ³J. R. Heflin, K. Y. Wong, O. Zamani-Khamiri, and A. F. Garito, *Phys. Rev. B* **38**, 1573 (1988); A. F. Garito, J. R. Heflin, K. Y. Wong, and O. Zamani-Khamiri, in *Nonlinear Optical Properties of Polymers*, edited by A. J. Heeger, J. Orenstein, and D. R. Ulrich, MRS Symposium Proceedings No. 109 (Material Research Society, Pittsburgh, 1988), p. 91.
- ⁴Z. G. Soos and S. Ramesha, *J. Chem. Phys.* **90**, 1067 (1989).
- ⁵C. P. DeMelo and R. Silbey, *Chem. Phys. Lett.* **140**, 537 (1987); *J. Chem. Phys.* **88**, 2567 (1988).
- ⁶R. Silbey, in *Conjugated Polymeric Materials: Opportunities in Electronics, Optoelectronics, and Molecular Electronics* [Ref. 1(b)], p. 1.
- ⁷S. N. Dixit, Dandan Guo, and S. Mazumdar, *Phys. Rev. B* **43**,

6781 (1991).

- ⁸Zhigang Shuai, D. Beljonne, and J. L. Brédas, *J. Chem. Phys.* (to be published).
- ⁹B. M. Pierce, *J. Chem. Phys.* **70**, 165 (1989); *Proc. SPIE* **1057** (1989).
- ¹⁰P. C. M. McWilliams, G. W. Hayden, and Z. G. Soos, *Phys. Rev. B* **43**, 9777 (1991).
- ¹¹P. C. M. McWilliams and Z. G. Soos, *J. Chem. Phys.* **95**, 2127 (1991).
- ¹²Z. G. Soos, G. W. Hayden, P. C. M. McWilliams, and S. Etemad, *J. Chem. Phys.* **93**, 7439 (1990).
- ¹³K. C. Rustagi and J. Ducuing, *Opt. Commun.* **10**, 258 (1974).
- ¹⁴H. F. Hameka, *J. Chem. Phys.* **67**, 2935 (1977); E. F. McIntyre and H. F. Hameka, *ibid.* **68**, 3481 (1978); **68**, 5534 (1978).
- ¹⁵E. F. McIntyre and H. F. Hameka, *J. Chem. Phys.* **69**, 4814 (1978); **70**, 2215 (1979); O. Zamani-Khamiri and H. F. Hameka, *ibid.* **71**, 1607 (1979); O. Zamani-Khamiri, E. F. McIntyre, and H. F. Hameka, *ibid.* **72**, 1280 (1980); **72**, 5906 (1980).
- ¹⁶J. Yu, B. Friedman, P. R. Baldwin, and W. P. Su, *Phys. Rev. B* **39**, 12 814 (1989); J. Yu, B. Friedman, and W. P. Su, in *Advanced Organic Solid State Materials*, edited by L. Y. Liang, P. M. Chaikin, and D. O. Cowan, MRS Symposium Proceedings No. 173 (Materials Research Society, Pittsburgh, 1990), p. 671.
- ¹⁷Weikang Wu, *Phys. Rev. Lett.* **61**, 1119 (1988).
- ¹⁸Changqin Wu and Xin Sun, *Phys. Rev. B* **41**, 12 845 (1990); **42**, 9736 (1990).
- ¹⁹Y. N. Genkin and P. M. Mednis, *Zh. Eksp. Teor. Fiz.* **54**, 1137 (1968) [*Sov. Phys.—JETP*, **27**, 609 (1968)].

- ²⁰Z. Shuai and J. L. Brédas, *Phys. Rev. B* **44**, 5962 (1991).
- ²¹W. P. Su, J. R. Schrieffer, and A. J. Heeger, *Phys. Rev. Lett.* **42**, 1698 (1979); *Phys. Rev. B* **22**, 2099 (1980).
- ²²(a) J. M. André, L. A. Burke, J. Delhalle, G. Nicolas, and Ph. Durand, *Int. J. Quantum Chem. Symp.* **13**, 283 (1979); (b) J. L. Brédas, in *Handbook of Conducting Polymers*, edited by T. A. Skotheim (Dekker, New York, 1986), Vol. 2, p. 859.
- ²³J. M. Toussaint, Ph. D. Thesis, University of Mons-Hainaut, 1991; J. M. Toussaint, F. Wudl, and J. L. Brédas, *J. Chem. Phys.* **91**, 1783 (1989); J. M. Toussaint and J. L. Brédas, *J. Chem. Phys.* **94**, 8122 (1991).
- ²⁴G. Nicolas and Ph. Durand, *J. Chem. Phys.* **70**, 2020 (1979).
- ²⁵J. L. Brédas, R. R. Chance, R. Silbey, G. Nicolas, and Ph. Durand, *J. Chem. Phys.* **75**, 255 (1981).
- ²⁶J. L. Brédas, R. R. Chance, R. Silbey, G. Nicolas, and Ph. Durand, *J. Chem. Phys.* **77**, 371 (1982).
- ²⁷E. Orti, J. L. Brédas, and C. Clarisse, *J. Chem. Phys.* **92**, 1228 (1990).
- ²⁸A. D. Buckingham, *Adv. Chem. Phys.* **12**, 107 (1967).
- ²⁹P. Pulay, *J. Chem. Phys.* **78**, 5043 (1983).
- ³⁰B. J. Orr and J. F. Ward, *Mol. Phys.* **20**, 513 (1971).
- ³¹J. Yu and W. P. Su, *Phys. Rev. B* **44**, 13 315 (1991).
- ³²S. J. Lalama and A. F. Garito, *Phys. Rev. A* **20**, 1179 (1979).
- ³³Z. G. Soos, G. W. Hayden, and P. C. M. McWilliams, in *Conjugated Polymeric Materials: Opportunities in Electronics, Optoelectronics, and Molecular Electronics* [Ref. 1(b)], p. 495.
- ³⁴The readers can find the diagrammatic representation of R-S perturbation in standard textbooks of quantum chemistry, for instance, A. Szabo and N. S. Ostlund, *Modern Quantum Chemistry* (Macmillan, New York, 1982), p. 331.
- ³⁵B. Hudson, B. E. Kohler, and K. Schulten, in *Excited States*, edited by E. C. Lim (Academic, New York, 1982), Vol. 6, p. 1. P. Tavern and K. Schulten, *Phys. Rev. B* **36**, 4337 (1987).
- ³⁶M. J. S. Dewar and W. J. Thiel, *J. Am. Chem. Soc.* **99**, 4899 (1977).
- ³⁷G. Hurst, M. Dupuis, and E. Clementi, *J. Chem. Phys.* **89**, 385 (1988).
- ³⁸H. A. Kurtz, *Int. J. Quantum Chem. Quantum Chem. Symp.* **24**, 791 (1990).
- ³⁹G. P. Agrawal, C. Cojan, and C. Flytzanis, *Phys. Rev. B* **17**, 776 (1978).
- ⁴⁰T. C. Kavanaugh and R. J. Silbey, *J. Chem. Phys.* **95**, 6924 (1991).
- ⁴¹Z. Shuai, D. Beljonne, and J. L. Brédas, *Solid State Commun.* **78**, 477 (1991).
- ⁴²T. Kaino *et al.*, *Electron. Lett.* **23**, 1095 (1987).
- ⁴³D. Li, T. J. Marks, and M. A. Ratner, *Chem. Phys. Lett.* **131**, 370 (1986); D. Li, M. A. Ratner, and T. J. Marks, *J. Am. Chem. Soc.* **110**, 1707 (1988).
- ⁴⁴D. McBranch, M. Sinclair, A. J. Heeger, A. O. Patil, S. Shi, and F. Wudl, *Synth. Met.* **29**, E85 (1989); D. D. C. Bradley and Y. Mori, *Jpn. J. Appl. Phys.* **28**, 174 (1989).
- ⁴⁵O. M. Gelsen, D. D. C. Bradley, H. Murata, N. Takada, T. Tutsui, S. Saito, and G. Leising, in *Electronic Properties of Polymers: Orientation and Dimensionality of Conjugated Systems*, edited by H. Kuzmany, M. Mehring, and S. Roth, Springer Series in Solid State Sciences Vol. 107 (Springer, Berlin, 1992), p. 221.
- ⁴⁶M. Dory, V. P. Bodart, J. Delhalle, J. M. André, and J. L. Brédas, in *Nonlinear Optical Properties of Polymers*, MRS Symposium Proceedings No. 109 (Ref. 3), p.239. J. L. Brédas, M. Dory, B. Thémans, J. Delhalle, and J. M. André, *Synth. Met.* **28**, D533 (1989).
- ⁴⁷S. R. Marder, D. N. Beratan, and L. T. Cheng, *Science* **252**, 103 (1991).
- ⁴⁸F. Meyers, C. Adant, and J. L. Brédas, *J. Am. Chem. Soc.* **113**, 3715 (1991).
- ⁴⁹C. Adant and J. L. Brédas (unpublished).